ISSN 1063-7737, Astronomy Letters, 2011, Vol. 37, No. 5, pp. 358–366. © Pleiades Publishing, Inc., 2011.
Original Russian Text © V.N. Obridko, V.E. Chertoprud, 2011, published in Pis'ma v Astronomicheskiĭ Zhurnal, 2011, Vol. 37, No. 5, pp. 392–400.

Longitude Variations of Solar Magnetic Fields of Different Intensity in Cycle 23 as Inferred from the SOHO/MDI Data

V. N. Obridko* **and V. E. Chertoprud**

Pushkov Institute of Terrestrial Magnetism, Ionosphere, and Radio Wave Propagation, Russian Academy of Sciences, Troitsk

Abstract—SOHO/MDI magnetograms have been used to analyze the longitude distribution of the squared solar magnetic field $\langle B^2 \rangle$ in the activity cycle no. 23. The energy of the magnetic field ($\langle B^2 \rangle$) is shown to change with longitude. However, these variations hardly fit the concept of active longitudes. In the epochs of high solar activity, one can readily see a relationship between longitude variations of the medium-strong (($|B| > 50$ G or $|B| > 100$ G) and relatively weak ($|B| \leq 50$ G or $|B| \leq 100$ G) fields at all latitudes. In other periods, this relationship is revealed mainly at the latitudes not higher than 30°. The background fields ($|B| \leq 25$ G) also display longitude variations, which are, however, not related to those of the strong fields. This makes us think that the fields of solar activity are rather inclusions to the general field than the source of the latter.

DOI: 10.1134/S1063773711050057

Keywords: *magnetic fields in the Sun.*

1. INTRODUCTION

The knowledge of the relationship between the local and so called background fields is of paramount importance for understanding the nature and mechanisms of generation of the magnetic field in the Sun. Two alternative hypotheses are available at present. The first one claims that background fields form part of the deep-rooted large-scale fields. These global fields are generated in the tachocline at the depth of 0.72 solar radii. The strong local fields are manifestations of the same mechanism, perhaps, intensified additionally in the surface layers. Therefore, the variations of strong local fields follow with a certain time delay those of background fields (Makarov and Mikhailutsa 1992; Makarov and Tlatov 1999, 2000; Makarov et al. 2001). Some authors supporting this hypothesis (e.g., Jouve et al. 2008, Lefebvre and Kosovichev 2005) believe that the original large-scale field is not deep-rooted, but, anyway, a time shift must exist between the background and local fields, and their general patterns must differ. According to the second hypothesis, the background fields are the product of decay of the local fields and the building material for the following cycle (Wang et al. 2009). In this case, one might expect a time shift in the opposite direction and a close similarity between the fields of different intensity in their distribution over the solar surface.

The situation is additionally complicated by the definition of the basic terms, which is not always unambiguous. Traditionally, the local fields are the magnetic fields of sunspots. Their intensity exceeds 2000 G. However, it would be more sensible to define local fields as the fields of active regions. The intensity of these fields (faculae, plages, pores, and micropores) ranges from hundreds of Gauss to $(1–2) \times 10^3$ G. The question of the minimum strength of local fields is of great importance to the dynamo theory. As shown in early publications, the field at the boundary of a calcium plage is 25 G and increases rapidly while moving inside the plage to its brighter parts (Skumanich et al. 1975). This was confirmed later by high-resolution measurements (Riehokainen et al. 2003), which gave the minimum field values equal to 25–50 G.

The internal structure of local and background fields is a special problem. In the sunspot umbra, where the field is strongest, it is mainly radial. There is reason to believe that active regions contain "kilogauss" tubes of the mainly radial field. However, the field direction in the faculae in the vicinity of sunspots is virtually unknown. The direct measurements of transverse fields in the faculae available so far are unreliable. On the other hand, the background fields turned out to be mostly transversal (Harvey et al. 2007, Ioshpa et al. 2009).

And finally, another unsolved problem is the spatial location of the local and background fields. The local

*E-mail: obridko@izmiran.ru

Table 1. Mean values of $\langle B^2 \rangle$ [G^2] for each intensity level in the aforementioned latitude ranges

	$\lvert B\rvert \le 25$ G	$\lvert B\rvert \le 50$ G	$\lvert B\rvert \le 100$ G	$\lvert B\rvert > 50$ G	$\lvert B\rvert > 100$ G	$B_{\rm all}$
NN1	178.6	396.6	492.2	7800	34442	818
N1	174.7	386.7	561.6	30437	64106	4693
C1	165.1	355.2	454.6	17101	43015	1673
S1	181.5	428.3	624.9	29448	67601	4586
SS1	192.6	506.6	721.9	6733	32485	1032
NN2	180.1	413.3	525.7	8824	32912	832
N2	178.5	422.8	710.7	53062	94629	9688
C2	172.3	402.8	651.3	58922	103194	9975
S2	185.8	473.1	800.8	50708	97176	10149
SS2	194.9	539.4	817.9	7407	30222	1237
NN3	178.5	397.1	479.7	5931	29172	577
N3	174.1	385.3	552.0	29987	62593	3793
C3	169.7	381.2	564.3	47598	87868	6467
S3	184.6	458.7	704.5	31137	68621	5468
SS3	195.6	541.4	809.0	5054	23373	919
NN4	177.1	383.5	448.9	4809	57233	475
N4	170.9	352.8	432.5	9434	29883	618
C4	165.2	350.9	446.0	17018	41484	1447
S4	182.8	431.2	574.0	8961	31616	930
SS4	195.0	524.3	752.8	4514	24827	802

fields are situated mainly in the central ("royal") zone at the latitudes of $\pm 30°$. Whether background fields exist also in this zone or only at higher latitudes is still not clear.

2. RELATIVELY WEAK AND MEDIUM-STRONG MAGNETIC FIELDS

SOHO/MDI magnetograms were used to analyze the longitude distribution of the squared solar magnetic field $\langle B^2 \rangle$. We considered a 14-year-long series of daily maps (1996.05–2009.09) with a band along the central meridian 101 pixels wide concentric with the solar disk chosen as the watch window.

The calculations were performed in five latitude ranges: $|\phi| < 13°$(C), $\phi \approx 13° - 32°$(N and S), and $\phi \approx 32° - 64°$(NN and SS) for four successive time intervals.

(1) Rise phase of cycle 23 (May 1, 1996–December 12, 1999).

(2) Maximum of cycle 23 (December 12, 1999–September 17, 2002).

(3) Decline of cycle 23 (September 18, 2002–April 10, 2006).

(4) Minimum 23–24 (April 11, 2006–September 30, 2009).

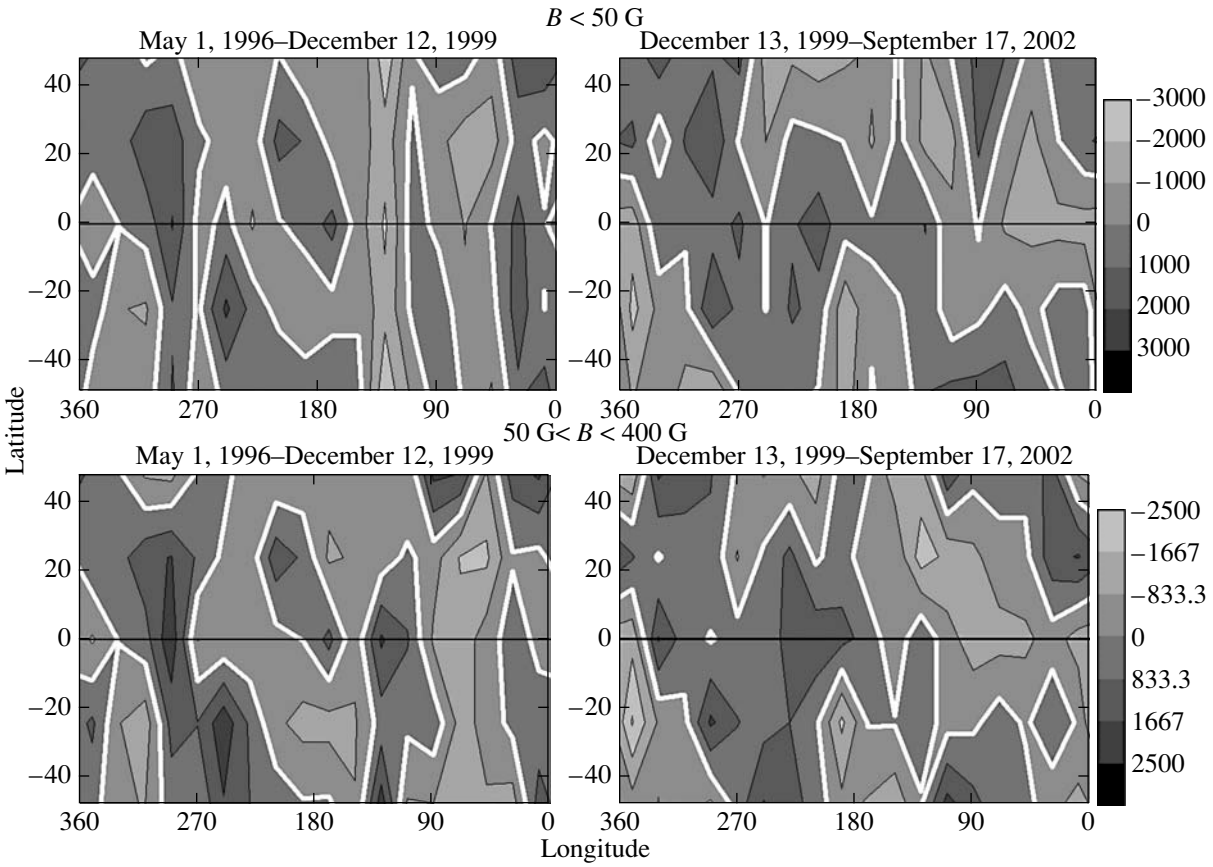

Fig. 1. Latitude-longitude diagrams for the periods of rising activity (May 1, 1996–December 12, 1999) and maximum of cycle 23 (December 13, 1999–September 17, 2002) for the relatively weak (upper panel) and medium-strong fields (lower panel).

The $\langle B^2 \rangle$ estimates obtained separately for each latitude interval on each magnetogram were averaged over all magnetograms relevant to the given longitude and time interval 18 longitude intervals were considered; i.e., the step in longitude was 20°. Intermediate information of three types was used: the plots of longitude variation of $\langle B^2 \rangle$ in different ranges of the magnetic field intensity, latitude-longitude diagrams of $\langle B^2 \rangle$ for relatively weak and medium-strong fields, and correlation estimates.

The longitude variations of $\langle B^2 \rangle$ for six levels of the magnetic field were studied in detail ($|B| \leq 25$ G, $|B| \leq 50$ G, $|B| \leq 100$ G, $|B| > 50$ G, $|B| > 100$ G, and all B (B_{all})) (see Table 1).

For compatibility, the longitude variations in Figs. 1–6 are given in standardized form, i.e., after the transformation

$$X \to st = [X - m(X)]/s(X),$$

where $m(X)$ and $s(X)$ are the mean value and standard deviation of the quantity X determined from the data for 18 longitudes.

Figures 1 and 2 illustrate the standardized values of $\langle B^2 \rangle$ multiplied by 1000 for $|B| \leq 50$ G and 50 G < $|B| \leq 400$ G for the fore time intervals mentioned above.

Figure 1 shows the latitude-longitude diagrams for the periods of increasing solar activity (May 1, 1996–December 12, 1999) and the maximum of cycle 23 (December 13, 1999–September 17, 2002) for the relatively weak (upper panel) and medium-strong (lower panel) fields. Fig. 2 represents the latitude–longitude diagrams for the periods of declining activity of cycle 23 (September 18, 2002–April 10, 2006) and minimum 23–24 (April 11, 2006–September 30, 2009) for the relatively weak (upper panel) and medium-strong (lower panel) fields.

The diagrams do not reveal any durable active longitudes. On the other hand, one can readily see that the diagrams for the relatively weak and medium-strong fields are similar in the periods of high solar activity (the maximum, declining phase, and, partly, the rise phase). At the minimum of the cycle, the similarity decreases; however, a correlation is still noticeable between the longitude variations of the medium-strong ($|B| > 50$ G, $|B| > 100$ G) and relatively weak ($|B| \leq 50$ G, $|B| \leq 100$ G) fields, though

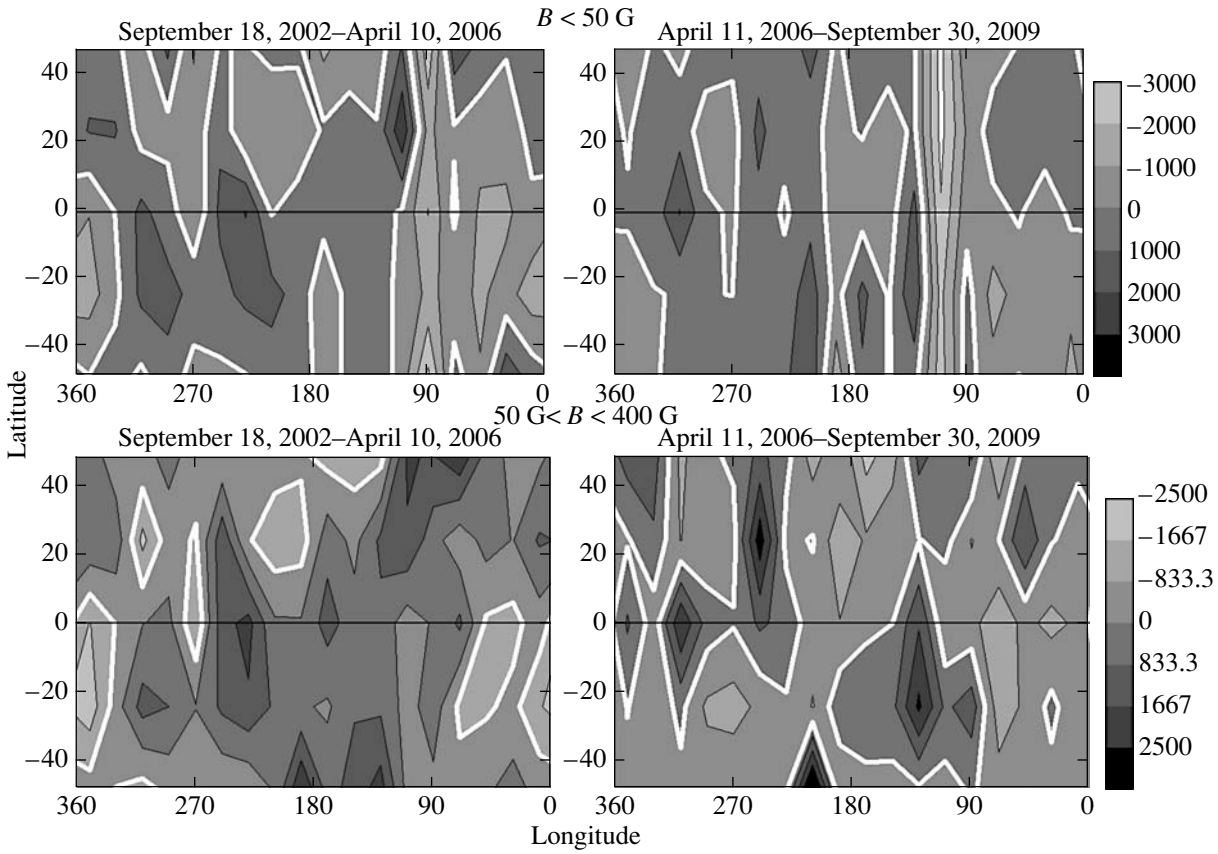

Fig. 2. Latitude-longitude diagrams for the declining phase of cycle 23 (September 18, 2002–April 10, 2006) and minimum 23–24 (April 11, 2006–September 30, 2009) for the relatively weak (upper panel) and medium-strong fields (lower panel).

only at the latitudes not exceeding ≈30°. The correlation coefficient is $R(|B| \leq 50$ G, $|B| > 50$ G$) = 0.53 \pm 0.12$. At higher latitudes, in the epoch of minimum, the similarity disappears simply because there are no medium-strong fields there at all.

This is demonstrated quantitatively by Table 2, which gives the correlation coefficients for longitude variations of the weak and medium- strong fields (see columns 5–8). The values in bold italics correspond to the maximum and declining phase of cycle 23. The last line gives the mean correlation coefficients for the periods of high activity obtained from ten estimates. As seen from Table 2, the correlation between longitude variations of the strong and weak fields becomes significant approximately at 30 G, and a limitation imposed on strong fields ($|B| \leq 400$ G) increases the correlation.

The gap in the table is due to the absence of data necessary to calculate the correlation coefficient. At high latitudes, observations of the magnetic field $|B| > 100$ G at the minimum of the cycle were scarce.

Turning back to the diagrams in Figs. 1 and 2, we should note that though they do not display any stable active longitudes, one can see a zone of decreased activity in the vicinity of the Carrington longitude of 90°–120°. This zone is particularly well pronounced on the diagrams for weak fields in the epochs of minimum and rising activity, though its traces are also noticeable on the other diagrams. The origin of this zone is not clear.

Longitude variations exist also at the level $|B| \leq 25$ G, but they are not related to the variations of strong fields. The correlation coefficient is $R(|B| \leq 25$ G, $|B| > 50$ G$) = 0.05 \pm 0.06$.

A few longitude dependences of $\langle B^2 \rangle$ from the hundreds analyzed are shown by way of example in Figs. 3–5. All of them refer to the maximum of cycle 23. Compared are the dependences for the fields $|B| \leq 25$ G and $|B| > 50$ G (Fig. 3) or for the fields $|B| \leq 50$ G and $|B| > 50$ G (Figs. 4 and 5). Examining the figures, we arrive at the following three conclusions corroborated by the correlation analysis (see Table 2):

1. The longitude variations of $\langle B^2 \rangle$ in all figures are not the result of observation errors.

2. The structure of these variations does not fit the concept of active longitudes (no clearly defined active longitudes are detected)

Table 2. Correlation between longitude variations $\langle B^2 \rangle$ for $|B| \le b_0$ and $b_0 < |B| \le 400$ G (columns 2–6) or for $|B| \le B_0$ and $|B| > B_0$ (columns 7 and 8)

	$b_0 = 25$	$b_0 = 30$	$b_0 = 35$	$b_0 = 40$	$b_0 = 50$	$B_0 = 50$	$B_0 = 100$
1	2	3	4	5	6	7	8
NN1	0.29	0.39	0.46	0.50	0.59	0.43	0.26
N1	0.67	0.57	0.81	0.90	0.93	0.88	0.88
C1	−0.09	−0.24	−0.03	0.22	0.43	0.65	0.60
S1	0.37	0.35	0.58	0.65	0.75	0.78	0.74
SS1	−0.67	−0.70	−0.53	−0.39	−0.10	−0.46	0.01
NN2	**0.08**	**0.42**	**0.48**	**0.56**	**0.49**	**0.56**	**0.36**
N2	**0.15**	**0.14**	**0.26**	**0.36**	**0.57**	**0.28**	**0.34**
C2	**0.12**	**0.65**	**0.59**	**0.70**	**0.79**	**0.77**	**0.76**
S2	**0.54**	**0.55**	**0.67**	**0.86**	**0.95**	**0.59**	**0.42**
SS2	**0.13**	**0.59**	**0.54**	**0.49**	**0.64**	**0.50**	**0.58**
NN3	**−0.26**	**−0.13**	**0.05**	**0.17**	**0.26**	**0.42**	**0.43**
N3	**0.06**	**−0.02**	**0.24**	**0.45**	**0.69**	**0.35**	**0.42**
C3	**0.58**	**0.48**	**0.32**	**0.54**	**0.71**	**0.23**	**0.42**
S3	**0.52**	**0.51**	**0.64**	**0.71**	**0.83**	**0.67**	**0.61**
SS3	**−0.28**	**0.01**	**0.39**	**0.35**	**0.24**	**0.24**	**0.23**
NN4	0.08	−0.16	−0.38	−0.41	−0.23	−0.13	–
N4	−0.14	−0.03	0.19	0.31	0.31	0.25	0.41
C4	0.23	0.29	0.25	0.35	0.66	0.44	0.46
S4	−0.01	0.08	0.07	0.20	0.30	0.17	0.46
SS4	0.18	0.40	0.50	0.51	0.50	0.26	−0.06
$\langle$**2, 3**$\rangle$	**0.164 ± .09**	**0.320 ± .09**	**0.418 ± .06**	**0.519 ± .06**	**0.617 ± .06**	**0.461 ± .06**	**0.457 ± .05**

3. In the periods of high solar activity, a distinct relationship exists between longitude variations of the relatively weak ($|B| \le 50$ G) and medium-strong ($|B| > 50$ G) magnetic fields, while the fields $|B| \le 25$ G and $|B| > 50$ G do not display such correlation.

Figure 3 shows longitude variations of the fields $|B| \le 25$ G and $|B| > 50$ G in the central latitude zone (C2) at the maximum of the activity cycle. The correlation is so low (0.03) that it can be considered absent at all.

In the Introduction, we have discussed the probability of time shifts in the distribution of weak and strong fields. Certain restrictions on these shifts follow from the estimates of correlation between longitude variations of the relatively weak ($|B| \le 50$ G) and medium-strong ($50 \text{ G} < |B| \le 400$ G) fields relevant to different time intervals. Without the time

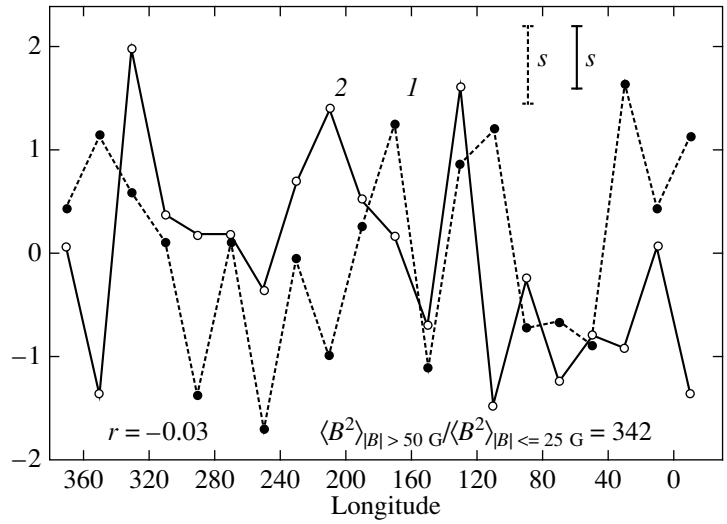

Fig. 3. Longitude variations of $\langle B^2\rangle$ at the maximum of cycle 23 in the central latitude zone (C2) for the fields $|B| \leq 25$ G (*1*) and $|B| > 50$ G (*2*). The variations are standardized.

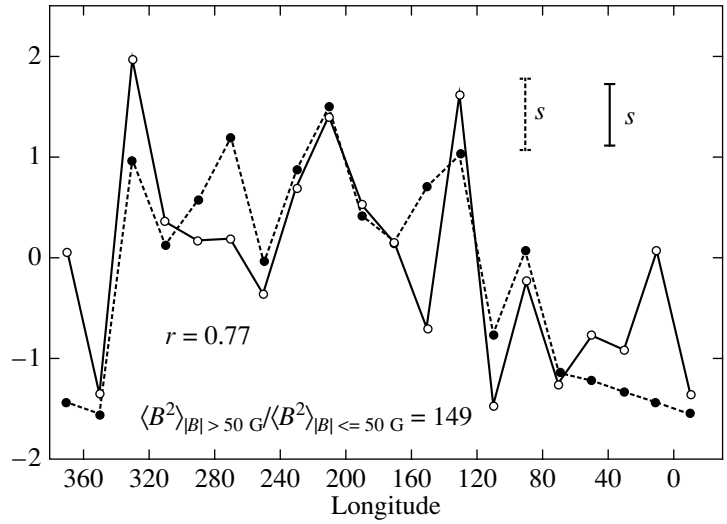

Fig. 4. Longitude variations $\langle B^2\rangle$ at the maximum of cycle 23 in the central latitude zone (C2) for the fields $|B| \leq 50$ G (*1*) and $|B| > 50$ G (*2*). The variations are standardized.

shift between the variations, the mean correlation coefficient is 0.51 ± 0.07. At a shift of 3–9 years, the correlation between longitude variations of these fields is insignificant (the maximum correlation coefficient does not exceed 0.16). The longitude variations of relatively weak fields in different time intervals (1, 2, 3, 4) are not correlated, as well as the variations of medium-strong fields analyzed in the same time intervals. This means that the general distribution of fields of different intensity over the solar surface is not conserved. Our results are likely to suggest that the relatively weak fields are not a mere product of decay of the strong fields.

On the other hand, very weak fields ($|B| \leq 25$ G), probably, form a separate population not related directly to the stronger fields.

3. STRONG MAGNETIC FIELDS

Now, we shall check the hypothesis that longitude variations of solar magnetic fields (or, more precisely, $\langle B^2\rangle$) are virtually identical for the weak and strong fields. In our considerations, we shall mean by strong fields the fields of sunspots with intensities more than 1 kG and by weak local fields, the fields of faculae with intensities from 100 to 1000 G.

The methods used to reveal the longitudinal structure differ for the strong and weak fields. The fact is

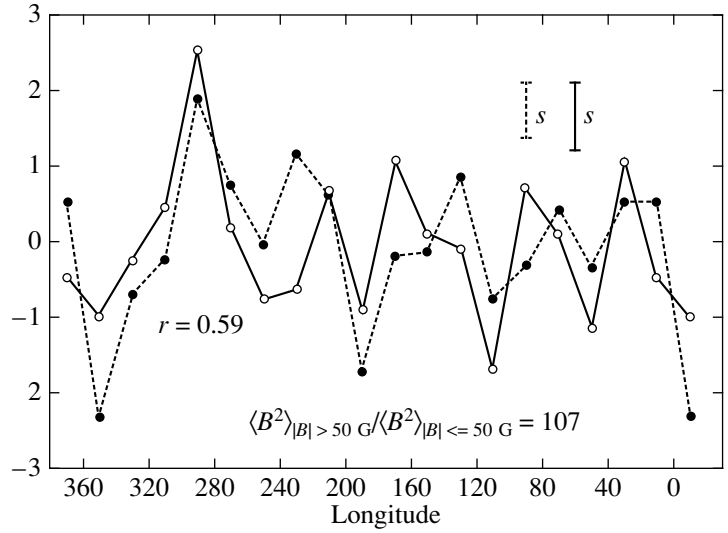

Fig. 5. Longitude variations $\langle B^2\rangle$ at the maximum of cycle 23 at the latitudes $\phi \approx 13^\circ - 32^\circ S$ (S2) for the fields $|B| \leq 50$ G (*1*) and $|B| > 50$ G (*2*). The variations are standardized.

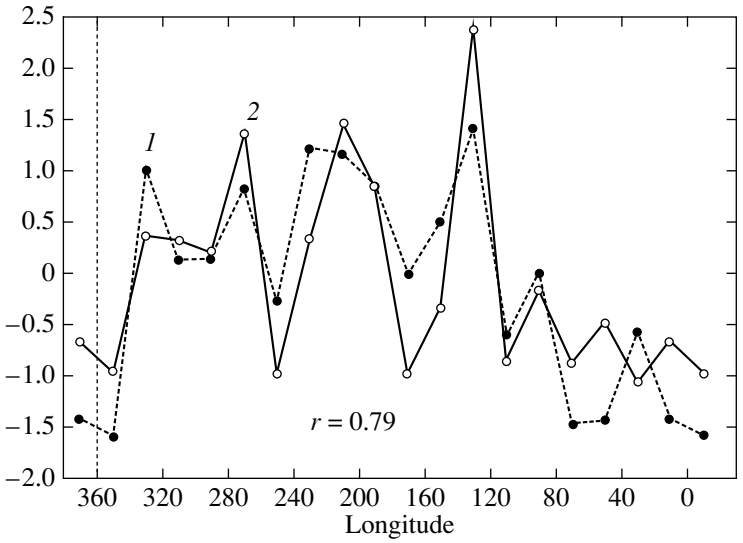

Fig. 6. Longitude variations of the index $S = \sum B^2$ at the maximum of cycle 23 in the central latitude zone (C2) for the fields $|B| \leq 100$ G (*1*) and $|B| > 2.8$ kG (*2*). The variations are standardized.

that if the strong fields are eliminated by the condition $|B| \leq b_0$, the number of points N in the watch window decreases insignificantly and exceeds a few thousands even at $b_0 \sim 10$ G. What is still more important, it does not virtually depend on longitude. On the contrary, if we consider the strong fields isolated by the condition $|B| > B_0$, the number of points in the watch window decreases dramatically (probably, down to zero) and can change significantly with longitude. In the former case, the values $S = \sum B^2$ and $\langle B^2\rangle = S/N$ are virtually proportional, and the choice of index for revealing the longitude structure of magnetic fields is not critical. The same is true for the results obtained from all data without limitations. In the latter case, the estimate of $\langle B^2\rangle$ (if any) is not necessarily proportional to the estimate of S. Moreover, the values $\langle B^2\rangle$ and S carry different information on the activity. The first one ($\langle B^2\rangle$) is proportional to the magnetic energy per unit area of the active features (determined from the criterion $|B| > B_0$). It need not change significantly with longitude or phase of the activity cycle. (By analogy, the mean area of large sunspots depends little on longitude and phase of the cycle). The second value (S) is proportional to the total magnetic energy of strong fields and, to a certain extent, to the total sunspot area in the given range

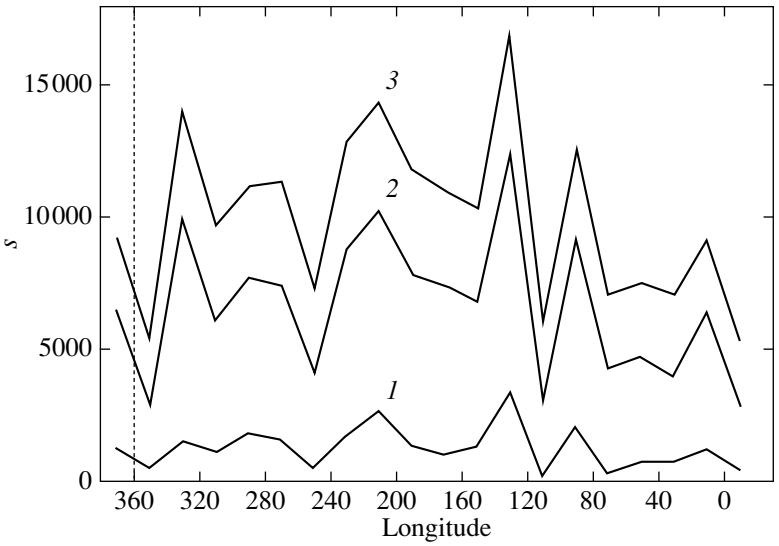

Fig. 7. Longitude variations of the index $S = \sum B^2$ at the of cycle 23 in the central latitude zone (C2) for the fields $|B| > 2$ kG (*1*), $|B| > 0.5$ kG (*2*) and arbitrary fields (*3*).

of latitudes, longitudes, and times. One should also bear in mind that the strong kilogauss fields in the SOHO/MDI data are underestimated.

In view of the aforesaid, we calculated the sum $S = \sum B^2$ in the given latitude, longitude, and time intervals to reveal the longitude structure of strong magnetic fields. Note that the number of observation days may differ at different longitudes due to gaps in the SOHO/MDI data, which was taken into account by introducing a weighting factor.

Figures 6 and 7 illustrate the longitude distribution of S for $|\phi| < 13°$ and $t \approx 2000-2002$ in different ranges of the magnetic field intensity.

As seen from Fig. 6, the longitude variations of the medium-strong ($|B| \leq 100$ G) and very strong ($|B| > 2800$ G) magnetic fields correlate fairly well ($r = 0.79$). Figure 7 shows that the longitude variations of strong fields are similar at different field intensities. The kilogauss fields correlate well at all latitudes and in all time intervals. The relationship between the strong, kilogauss fields and weaker fields of the faculae is more complicated. In the rise phase, all fields display a good correlation at the equator. At the maximum and in the declining phase, the strong and weak fields (particularly, very strong and very weak ones) correlate poorly at all latitudes.

4. CONCLUSIONS

1. The energy of the magnetic field ($\langle B^2 \rangle$) changes with longitude. However, the pattern of these variations hardly fits the concept of active longitudes. No specific longitudes are detected except for a narrow band of $100°-200°$ where the activity is absent at the beginning and the end of the cycle, and a certain similarity of the general structure of weak fields. The longitudinal "pattern" does not last long.

2. The longitude variations of medium-strong ($|B| > 50$ G or $|B| > 100$ G) and relatively weak ($|B| \leq 50$ G or $|B| \leq 100$ G) fields display a pronounced correlation at all latitudes in the periods of high solar activity. The mean values of 10 correlation coefficients in these periods (bold italics in Table 2) are: $R(|B| \leq 50\ \text{G},\ |B| > 50\ \text{G}) = 0.46 \pm 0.06$, $R(|B| \leq 100\ \text{G},\ |B| > 100\ \text{G}) = 0.46 \pm 0.05$. At the maximum of the cycle, the correlation decreases as we move away from the equatorial zone (particularly, in the northern hemisphere), and the active longitudes can hardly be isolated. In the rise phase, the correlation is high at all latitudes up to 35°, and some evidence of active longitudes is noticeable in the vicinity of $240°-300°$. In the declining phase, the correlation is low in the central zone and high at mid latitudes. The active longitudes can be identified in the vicinity of 100° in the northern hemisphere and at $240°-300°$ in the southern hemisphere.

3. A correlation of longitude variations of the medium-strong and relatively weak fields exists also in the epochs of low activity, but it is mainly observed at the latitudes not higher than ≈30°. $R(|B| \leq 50\ \text{G},\ |B| > 50\ \text{G}) = 0.53 \pm 0.12$.

4. As seen from Table 2, the correlation between the strong and weak fields becomes significant at approximately 30 G, increasing under the limiting condition ($|B| \leq 400$ G). The fields $|B| \leq 25$ G also display longitude variations, but they are not related to those of strong fields. $R(|B| \leq 25\ \text{G},\ |B| > 50\ \text{G}) = 0.05 \pm 0.06$.

Of fundamental importance to modeling the structure and evolution of solar magnetic fields is the conclusion of nearly synchronous longitude variations of index S calculated for the fields of different intensities ($|B| \leq 100$ G and $|B| > B_0$, where $B_0 = 0-2800$ G). Taking into account the results of Section 1, we can say that energy variations of the fields of different intensities (from 50 to 3000 G) are similar. In this context, it seems correct to suggest that the fields of solar activity are mere inclusions to the general field rather that being its source.

5. ACKNOWLEDGMENTS

The work was supported by the Russian Foundation for Basic Research, project no. 08-02-00070. The authors are grateful to the SOHO/MDI team for the data.

REFERENCES

1. J. W. Harvey, D. Branston, C. J. Henney, C. U. Keller, SOLIS and GONG Teams. Astrophysical Journal, Volume 659, Issue 2, pp. L177-L180. (2007)
2. B. A. Ioshpa, V. N. Obridko, V. E. Chertoprud, Pisma Astron. Zh., **36**(6), 472 (2009).
3. L. Jouve, A. S. Brun, R. Arlt, A. Brandenburg, M. Dikpati, A. Bonanno, P. J. Кдруlд, D. Moss, M. Rempel, P. Gilman, M. J. Korpi, A. G. Kosovichev, Astron. Astrophys. **483**, Issue 3, 949 (2008).
4. S. Lefebvre, A. G. Kosovichev, Astrophys. J., **633**, Issue 2, L149-L152 (2005).
5. V. I. Makarov, V. P. Mikhallutsa, The solar cycle; Proceedings of the National Solar Observatory/Sacramento Peak 12th Summer Workshop, ASP Conference Series (ASP: San Francisco), vol. 27, p. 404. (1992)
6. V. I. Makarov, A. G. Tlatov, The 9th European Meeting on Solar Physics, held 12-18 September, 1999, in Florence, Italy. Edited by A. Wilson. European Space Agency, ESA SP-448, ISBN: 92-9092-792-5., p. 125 (1999).
7. V. I. Makarov, A. G. Tlatov, J. Astrophys. Astron. **21**, 161 (2000).
8. V. I. Makarov, A. G. Tlatov, D. K. Callebaut, V. N. Obridko, and B. D. Shelting, Solar Physics **198**, 409 (2001)
9. A. Riehokainen, E. Valtaoja, S. Pohjolainen, Astron. and Astrophys. **402**, 1103 (2003).
10. A. Skumanich, C. Smythe, E. N. Frazier, Astrophys. J. **200**, Sept. 15, pt. 1, 747 (1975).
11. Y.-M. Wang, E. Robbrecht, N. R. Sheeley, Astrophys. J., **707**, Issue 2, 1372 (2009).